



Impacts of Dust Grains Accelerated by Supernovae on the Moon

Amir Siraj¹ and Abraham Loeb¹

Department of Astronomy, Harvard University, 60 Garden Street, Cambridge, MA 02138, USA; amir.siraj@cfa.harvard.edu, aloeb@cfa.harvard.edu
 Received 2020 April 23; revised 2020 May 14; accepted 2020 May 16; published 2020 June 2

Abstract

There is evidence that ejecta from nearby supernovae have rained down on Earth in the past. Supernovae can accelerate preexisting dust grains in the interstellar medium to speeds of $\sim 0.01c$. We investigate the survival and impact of dust grains from supernovae on the Moon, finding that supernova dust grains can form detectable tracks with widths of $\sim 0.01\text{--}0.07\ \mu\text{m}$ and depths of $\sim 0.1\text{--}0.7\ \text{mm}$ in lunar rocks. These tracks could potentially shed light on the timings, luminosities, and directions of nearby supernovae.

Unified Astronomy Thesaurus concepts: [Supernovae \(1668\)](#); [The Moon \(1692\)](#); [Meteoroids \(1040\)](#)

1. Introduction

There is evidence that nearby supernovae have resulted in the ^{60}Fe and other radionuclides detected in deep-ocean samples (Knie et al. 1999, 2004; Feige et al. 2012; Wallner et al. 2016), the lunar surface (Fimiani et al. 2016), cosmic rays (Ruderman 1974; Kachelrieß et al. 2015, 2018), and microfossils (Ludwig et al. 2016). Supernovae ejecta can accelerate dust to subrelativistic speeds $\lesssim 0.1c$ (Spitzer 1949; Bingham & Tsyvovich 1999; Weiler 2003; Hoang et al. 2015). Studying dust accelerated by supernovae could elucidate the history of nearby supernovae (Knie et al. 2004; Thomas et al. 2016; Wallner et al. 2016; Melott et al. 2017) and constrain theoretical models of supernovae (Wesson et al. 2015; Bevan et al. 2017; De Looze et al. 2017; Kirchsclager et al. 2019). Searches on the lunar surface for signatures from interstellar objects have been suggested (Lingam & Loeb 2019; Siraj & Loeb 2020a). Dust grains accelerated by supernovae could appear as meteors in the Earth’s atmosphere (Siraj & Loeb 2020b) and as chemical enrichments in subsurface layers on the Moon (Crawford 2017). Given that NASA’s Artemis program plans to establish a sustainable base on the Moon by 2024,¹ it is now particularly timely to explore the detection signatures of interstellar dust on its regolith and rocks. In this Letter, we explore the flux of dust grains accelerated by supernovae at the lunar surface and the expected rate of the resulting impact tracks in lunar materials.

Our discussion is structured as follows. In Section 2, we consider the survival of dust grains accelerated by supernovae as they travel to the Moon. In Section 3, we investigate the effect of radiation pressure from supernovae on the acceleration of dust grains. In Section 4, we explore the lunar impact rate of such dust grains. In Section 5, we estimate the depth to which these dust grains penetrate lunar materials. In Section 6, we compute the expected track densities in lunar rocks. Finally, in Section 7 we summarize key predictions and implications of our model.

2. Grain Survival

Coulomb explosions from charge accumulation hinder the distance that supernova dust grains can travel in the interstellar medium (ISM). The surface potential ϕ_{max} above which the grain will be disrupted by Coulomb explosions, assuming a

typical tensile strength of $\sim 10^{10}\ \text{dyn cm}^{-2}$, is (Hoang et al. 2015)

$$e\phi_{\text{max}} \simeq 0.1\ \text{keV} \left(\frac{r}{0.01\ \mu\text{m}} \right), \quad (1)$$

where e is the electron charge. There is also a maximum surface potential $U_{\text{max,H}}$ due to the fact that a large potential can halt electrons from overcoming the surface potential and therefore escaping the grain (Hoang & Loeb 2017),

$$eU_{\text{max,H}} = 2m_e v^2 \simeq 0.1\ \text{keV} \left(\frac{v}{0.01c} \right)^2, \quad (2)$$

where m_e is the electron mass. Combining Equations (1) and (2)

$$\left(\frac{r}{0.01\ \mu\text{m}} \right) \gtrsim \left(\frac{v}{0.01c} \right)^2 \quad (3)$$

yields a minimum grain radius of $r \sim 0.01\ \mu\text{m}$ for survival at a speed of $v \sim 0.01c$ and implies that grains above this size will not undergo Coulomb explosions while traveling through the ISM.

Significant slow-down for dust grains traveling through the ISM occurs at distance where the total momentum transferred by particles in the ISM to the object is comparable to the initial momentum of the object. However, at the speed of $\sim 0.01c$, the stopping distance of a proton in silicate material is comparable to the size of the grain for a radius $r \sim 0.4\ \mu\text{m}$ (Figure 2 of Hoang et al. 2017), so the stopping distance through the ISM for $r \lesssim 0.4\ \mu\text{m}$ and $v \sim 0.01c$ is

$$d_{\text{ISM}} \sim 250\ \text{pc} \left(\frac{\rho}{3\ \text{g cm}^{-3}} \right) \left(\frac{n_p}{0.1\ \text{cm}^{-3}} \right)^{-1}, \quad (4)$$

given the local proton density of the ISM is $n_p \sim 0.1\ \text{cm}^{-3}$ (Frisch et al. 2011). At faster speeds, $d_{\text{ISM}} \gtrsim 250\ \text{pc}$, but this contribution does not significantly enhance the flux of dust grains from supernovae, so it is not studied here.

Additionally, thermal sublimation in both the ISM and the solar radiation field and Coulomb explosions in the solar wind do not limit further the sizes and speeds of grains considered here (Hoang et al. 2015). We note that interstellar dust particles of similar sizes considered here that travel at typical speeds are excluded from the inner solar system due to heliospheric and

¹ <https://www.nasa.gov/specials/artemis/>

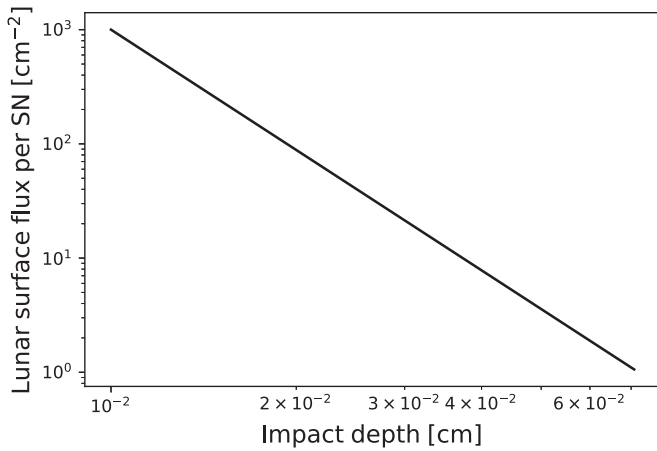


Figure 1. Lunar surface flux of dust grains as a function of impact depth, accelerated by a single supernova at ~ 250 pc. The range corresponds to grain sizes of ~ 0.01 – $0.07 \mu\text{m}$ and speeds of ~ 0.01 – $0.03c$.

radiation pressure effects (see Sterken et al. 2019 for a review on interstellar dust in the solar system).

3. Grain Acceleration

Radiation pressure from a supernova accelerates dust grains to subrelativistic speeds (Spitzer 1949; Bingham & Tsyto- vich 1999; Weiler 2003; Hoang et al. 2015). Assuming a typical bolometric luminosity of $\sim 10^8 L_\odot$, Equation (12) in Hoang et al. (2015) yields

$$v \sim 0.01c \left(\frac{d}{5 \times 10^{18} \text{ cm}} \right)^{-1/2} \left(\frac{r}{0.01 \mu\text{m}} \right)^{-1/2}, \quad (5)$$

where r is the grain radius, d is the initial distance, and v is the grain speed. Since dust grains are sublimated within a distance of $d \sim 10^{16}$ cm, Equations (3) and (5) jointly constrain the range of sizes that this method is applicable to grains of size ~ 0.01 – $0.07 \mu\text{m}$, corresponding to speeds of ~ 0.01 – $0.03c$.

Adopting the canonical dust mass fraction in the ISM of ~ 0.01 , $\sim 2 \times 10^{-4} M_\odot$ of preexisting dust around each supernova exists within a distance of 5×10^{18} cm, interior to which $r \sim 0.01 \mu\text{m}$ dust grains can be accelerated to $\sim 0.01c$. The fraction of ISM dust with size $r \gtrsim 0.01 \mu\text{m}$ is ~ 0.5 (Mathis et al. 1977), so $\sim 10^{-4} M_\odot$ of dust is accelerated per supernova, corresponding to $\sim 10^{44}$ grains. Additionally, the size distribution of ISM dust grains follows a power law with exponent -3.5 (Mathis et al. 1977).

Dust grains produced in supernovae travel at the ejecta speed of $\sim 0.01c$ because the drag timescale due to gas (Sarangi & Cherchneff 2015) is short relative to the acceleration timescale by radiation pressure (Hoang et al. 2017). However, the abundance and size distribution of supernova ejecta dust are model dependent, unlike preexisting dust grains in the ISM. The ejecta model for typical Type II-P supernovae, presented in Figure 4 of Sarangi & Cherchneff (2015), peaks for grain radii of $r \sim 0.02 \mu\text{m}$, a size bin at which $\sim 5 \times 10^{-3} M_\odot$ of dust grains is produced per supernova, which also corresponds to $\sim 10^{44}$ grains. Further modeling of the ejecta of core-collapse supernovae in general will reveal the true abundance of subrelativistic dust grains produced relative to preexisting ISM dust that is accelerated by the radiation pressure of the supernova. Additionally, ejecta-formed dust likely undergo

different dynamics relative to accelerated ISM dust grains (Fry et al. 2018; Fields et al. 2019).

In addition, massive stars such as luminous blue variables can reach stellar wind mass-loss rates of $\sim 10^{-5} M_\odot \text{ yr}^{-1}$ (Andrews et al. 2011), which could lead to $\sim 10^{-4} M_\odot$ of preexisting dust that would be accelerated to $\gtrsim 0.01c$ due to radiation pressure from the supernova. However, luminous blue variables are a small fraction of all supernovae, so we do not consider them here.

4. Impact Rate

The local timescale between core-collapse supernovae is estimated to be $\tau_{\text{SN}} \sim 2$ Myr within a distance $d_{\text{SN}} \sim 100$ pc (Knie et al. 2004; Thomas et al. 2016; Wallner et al. 2016; Melott et al. 2017), implying a timescale of $\tau_{\text{SN}} \sim 0.1$ Myr within a distance $d_{\text{SN}} \sim 250$ pc.

SNE II are an order of magnitude more common than SNE Ib/c, and so we focus our discussion on them (Guetta & Della Valle 2007).

The impact area density on the lunar surface due to one supernova at ~ 250 pc of $r \sim 0.01 \mu\text{m}$ dust grains traveling at $\sim 0.01c$ accelerated by core-collapse supernovae is therefore

$$\sigma_{\text{SN}} \sim 10^3 \text{ cm}^{-2} \left(\frac{d_{\text{SN}}}{250 \text{ pc}} \right)^{-2} \left(\frac{\tau_{\text{SN}}}{0.1 \text{ Myr}} \right). \quad (6)$$

5. Impact Tracks

Lunar surface material is composed primarily of silicates (Keller & McKay 1997; Prettyman et al. 2006; Melosh 2007; Greenhagen et al. 2010), and so we adopt the properties of quartz for our impact depth penetration analysis. Since the impacts occur at subrelativistic speeds, we consider the dust grains as collections of constituent nuclei (Si, as a fiducial example). The stopping power dE/dx as a function of Si nucleus speed for impacts in quartz is adopted from Figure 2 of Hoang et al. (2017), allowing the penetration depth l of a single ion to be computed.

The sideways shock moves at a speed $\lesssim 10^{-2}$ of the dust speed, producing a “track” in which the depth greatly exceeds the width, which is comparable to the size of the dust grain. Only a fraction of the total energy is shared with the target per penetration depth of a single ion. This energy fraction ϵ is found by lowering the sideways speed v_{shock} per penetration depth x such that the timescale to traverse the dust grain radius r sideways, r/v_{shock} , equals the timescale to traverse the penetration depth l at the dust speed, l/v . This means that $v_{\text{shock}} = (rv/l)$, implying an energy deposition fraction, $\epsilon = r/l$. Since we deposit the fraction ϵ of the dust energy per penetration depth x , the total penetration depth is $D \sim l^2/r$.

With a grain radius of $r \sim 0.01 \mu\text{m}$ and a penetration depth per ion of $l \sim 1 \mu\text{m}$ the total penetration depth is $D \sim 0.1$ mm. The penetration depth for a constant size scales as $D \propto v^4$, since dE/dx is constant to order unity over the speeds considered; however, due to the size-speed constraint of Equation (3) and the fact that $D \propto r^{-1}$, the penetration depth actually scales as $dD/dv \propto v^2$. The abundance of dust grains, N , scales as the volume (d^3) multiplied by the ISM dust grain size distribution ($r^{-3.5}$). Since Equation (5) yields $rd \propto v^{-2}$ and Equation (3) gives $r \propto v^2$, in total the abundance scales as $dN/dv \propto v^{-5}$. As a function of depth, the abundance scales as

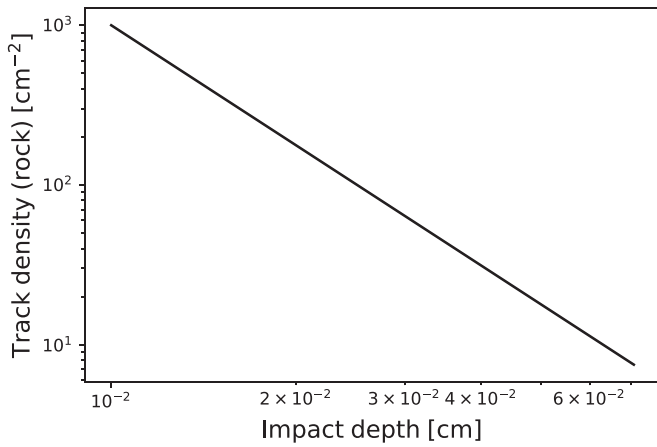


Figure 2. Current expected track density as a function of track depth in the lunar rock, resulting from impacts of dust grains with sizes of $\sim 0.01\text{--}0.07\ \mu\text{m}$ and speeds of $\sim 0.01\text{--}0.03c$. In contrast with Figure 1, this plot is corrected for the lunar rock erosion rate discussed in the text.

$dN/dD \propto v^{-7}$, which, using Equation (5), yields a total dependence of the dust grain flux at the lunar surface of $dN/dD \propto D^{-7/2}$, as indicated in Figure 1.

6. Signatures in Lunar Materials

The lunar regolith is steadily overturned by micrometeoroid impacts (see Grün et al. 2011 for a review of the lunar dust environment). The approximate depth D to which the lunar regolith is overturned as a function of timescale τ , given in Figure 9 of Costello et al. (2018), is

$$D \sim 10\text{ cm} \left(\frac{\tau}{0.1\text{ Myr}} \right)^{1/4}, \quad (7)$$

which implies that tracks resulting from the penetration of dust grains accelerated by nearby supernovae into the lunar regolith cannot be discovered, given that the overturned depth between supernovae within $\sim 250\text{ pc}$ is 1000 times larger than the track depth for $r \sim 0.01\ \mu\text{m}$ dust grains at $\sim 0.01c$.

Lunar rocks, on the other hand, are eroded by micrometeoroids at a rate of $\sim 0.1\text{--}1\text{ mm Myr}^{-1}$ (Comstock 1972; Neukum 1973; Fechtig et al. 1977; Nishiizumi et al. 1995; Eugster 2003; Eugster et al. 2006). We conservatively adopt a rate of $\sim 1\text{ mm Myr}^{-1}$. They have surface lifetimes of $1\text{--}50\text{ Myr}$ (Walker 1980; Heiken et al. 1991). Impact tracks can be discovered in lunar rocks at rates shown in Figure 2.

Micrometeoroid impacts result in craters with depths comparable to their widths, and cosmic rays develop tracks with widths of $\sim 1\text{ pm}$, so subrelativistic dust grain tracks are uniquely identifiable by their characteristic $\sim 0.01\ \mu\text{m}$ widths and depths that greatly exceed what would be expected from a micrometeoroid impact.

7. Discussion

We demonstrated that tracks resulting from $r \sim 0.01\text{--}0.07\ \mu\text{m}$ dust grains accelerated by supernovae to speeds of $r \sim 0.01\text{--}0.03c$ can be discovered in the lunar rocks. Studies of lunar rocks could shed light on the history of supernovae within the past $\sim 1\text{ Myr}$ and within $\sim 250\text{ pc}$, with the potential to reveal the timings, luminosities, and directions of recent supernovae. The expected density of tracks is

$\sim 10^3\text{ cm}^{-2}$ for depths of $\sim 0.1\text{ mm}$ and widths of $\sim 0.01\ \mu\text{m}$ and $\sim 1\text{ cm}^{-2}$ for depths of $\sim 0.7\text{ mm}$ and widths of $\sim 0.07\ \mu\text{m}$. However, since lunar rocks may be covered by regolith material with typical grain sizes of $\sim 100\ \mu\text{m}$ (Heiken et al. 1991), impacts of the subrelativistic grains considered here could catastrophically disrupt such grains instead of forming tracks within a rock, potentially reducing the actual density of tracks observed on lunar rocks.

The six Apollo missions brought to Earth 2200 lunar rocks² that could be searched for these tracks. While cosmic-ray tracks have been discovered in lunar samples (Droz et al. 1974; Crozaz 1980; Bhandari 1981), these tracks would be differentiable by their widths, which would be at least an order of magnitude larger. Extraterrestrial artifacts, such as microscopic probes akin to Breakthrough Starshot,³ could also form such tracks.

We thank Brian J. Fry and Thiem Hoang for helpful comments. This work was supported in part by a grant from the Breakthrough Prize Foundation.

ORCID iDs

Amir Siraj  <https://orcid.org/0000-0002-9321-6016>

Abraham Loeb  <https://orcid.org/0000-0003-4330-287X>

References

- Andrews, J. E., Clayton, G. C., Wesson, R., et al. 2011, *AJ*, **142**, 45
- Bevan, A., Barlow, M. J., & Milisavljevic, D. 2017, *MNRAS*, **465**, 4044
- Bhandari, N. 1981, *InEPS*, **90**, 359
- Bingham, R., & Tsytoich, V. N. 1999, *Aph*, **12**, 35
- Comstock, G. M. 1972, in *IAU Symp. 47, The Moon*, ed. S. K. Runcorn & H. C. Urey (Dordrecht: Reidel), 330
- Costello, E. S., Ghent, R. R., & Lucey, P. G. 2018, *Icar*, **314**, 327
- Crawford, I. A. 2017, in *Handbook of Supernovae*, ed. A. W. Alsabti & P. Murdin (Cham: Springer), 2507
- Crozaz, G. 1980, in *The Ancient Sun: Fossil Record in the Earth, Moon and Meteorites*, ed. R. O. Pepin, J. A. Eddy, & R. B. Merrill (New York: Pergamon), 331
- De Looze, I., Barlow, M. J., Swinyard, B. M., et al. 2017, *MNRAS*, **465**, 3309
- Droz, R. J., Hohenberg, C. M., Morgan, C. J., & Ralston, C. E. 1974, *GeCoA*, **38**, 1625
- Eugster, O. 2003, *ChEG*, **63**, 3
- Eugster, O., Herzog, G. F., Marti, K., & Caffee, M. W. 2006, in *Meteorites and the Early Solar System II*, ed. D. S. Lauretta & H. Y. McSween (Tucson, AZ: Univ. Arizona Press), 829
- Fechtig, H., Gentner, W., Hartung, J. B., et al. 1977, *NASSP*, **370**, 585
- Feige, J., Wallner, A., Winkler, S. R., et al. 2012, *PASA*, **29**, 109
- Fields, B., Ellis, J. R., Binns, W. R., et al. 2019, *BAAS*, **51**, 410
- Fimiani, L., Cook, D. L., Faestermann, T., et al. 2016, *PhRvL*, **116**, 151104
- Frisch, P. C., Redfield, S., & Slavin, J. D. 2011, *ARA&A*, **49**, 237
- Fry, B. J., Fields, B. D., & Ellis, J. R. 2018, arXiv:1801.06859
- Greenhagen, B. T., Lucey, P. G., Wyatt, M. B., et al. 2010, *Sci*, **329**, 1507
- Grün, E., Horanyi, M., & Sternovsky, Z. 2011, *P&SS*, **59**, 1672
- Guetta, D., & Della Valle, M. 2007, *ApJL*, **657**, L73
- Heiken, G. H., Vaniman, D. T., & French, B. M. 1991, *Lunar Sourcebook*, A User's Guide to the Moon (Cambridge: Cambridge Univ. Press)
- Hoang, T., Lazarian, A., Burkhart, B., & Loeb, A. 2017, *ApJ*, **837**, 5
- Hoang, T., Lazarian, A., & Schlickeiser, R. 2015, *ApJ*, **806**, 255
- Hoang, T., & Loeb, A. 2017, *ApJ*, **848**, 31
- Kachelrieß, M., Neronov, A., & Semikoz, D. V. 2015, *PhRvL*, **115**, 181103
- Kachelrieß, M., Neronov, A., & Semikoz, D. V. 2018, *PhRvD*, **97**, 063011
- Keller, L. P., & McKay, D. S. 1997, *GeCoA*, **61**, 2331
- Kirchschlager, F., Schmidt, F. D., Barlow, M. J., et al. 2019, *MNRAS*, **489**, 4465
- Knie, K., Korschinek, G., Faestermann, T., et al. 1999, *PhRvL*, **83**, 18

² <https://curator.jsc.nasa.gov/lunar/>

³ <https://breakthroughinitiatives.org/initiative/3>

- Knie, K., Korschinek, G., Faestermann, T., et al. 2004, *PhRvL*, **93**, 171103
- Lingam, M., & Loeb, A. 2019, arXiv:1907.05427
- Ludwig, P., Bishop, S., Egli, R., et al. 2016, *PNAS*, **113**, 9232
- Mathis, J. S., Rimpl, W., & Nordsieck, K. H. 1977, *ApJ*, **217**, 425
- Melosh, H. J. 2007, *M&PS*, **42**, 2079
- Melott, A. L., Thomas, B. C., Kachelrieß, M., Semikoz, D. V., & Overholt, A. C. 2017, *ApJ*, **840**, 105
- Neukum, G. 1973, *LPSC*, **4**, 558
- Nishiizumi, K., Kohl, C. P., Arnold, J. R., et al. 1995, *LPSC*, **26**, 1055
- Prettyman, T. H., Hagerty, J. J., Elphic, R. C., et al. 2006, *JGRE*, **111**, E12007
- Ruderman, M. A. 1974, *Sci*, **184**, 1079
- Sarang, A., & Cherchneff, I. 2015, *A&A*, **575**, A95
- Siraj, A., & Loeb, A. 2020a, *AcAau*, **173**, 53
- Siraj, A., & Loeb, A. 2020b, arXiv:2002.01476
- Spitzer, L. 1949, *PhRv*, **76**, 583
- Sterken, V. J., Westphal, A. J., Altobelli, N., Malaspina, D., & Postberg, F. 2019, *SSRv*, **215**, 43
- Thomas, B. C., Engler, E. E., Kachelrieß, M., et al. 2016, *ApJL*, **826**, L3
- Walker, R. M. 1980, in *The Ancient Sun: Fossil Record in the Earth, Moon and Meteorites*, ed. R. O. Pepin, J. A. Eddy, & R. B. Merrill (New York: Pergamon), **11**
- Wallner, A., Feige, J., Kinoshita, N., et al. 2016, *Natur*, **532**, 69
- Weiler, K. 2003, *Supernovae and Gamma-Ray Bursters*, Lecture Note in Physics, Vol. 598 (Berlin: Springer)
- Wesson, R., Barlow, M. J., Matsuura, M., & Ercolano, B. 2015, *MNRAS*, **446**, 2089